

Characterization of LIGO 4-km Fabry-Perot cavities via high-frequency dynamic responses to length and laser frequency variations

M. Rakhmanov (UF), F. Bondu, O. Debieu (CNRS), and R. Savage (LIGO)

Introduction

The condition for resonance in a Fabry-Perot cavity in the presence of length and laser frequency variations is given by

$$C(s) \frac{\delta\tilde{\omega}(s)}{\omega} = -\frac{\delta\tilde{L}(s)}{L}, \quad \text{where} \quad C(s) = \frac{1 - e^{-2sT}}{2sT}.$$

Here T is the light transit time in the cavity and $C(s)$ is the normalized frequency-to-length transfer function (derivation can be found in *Phys. Lett. A* 305 (2002) p.239).

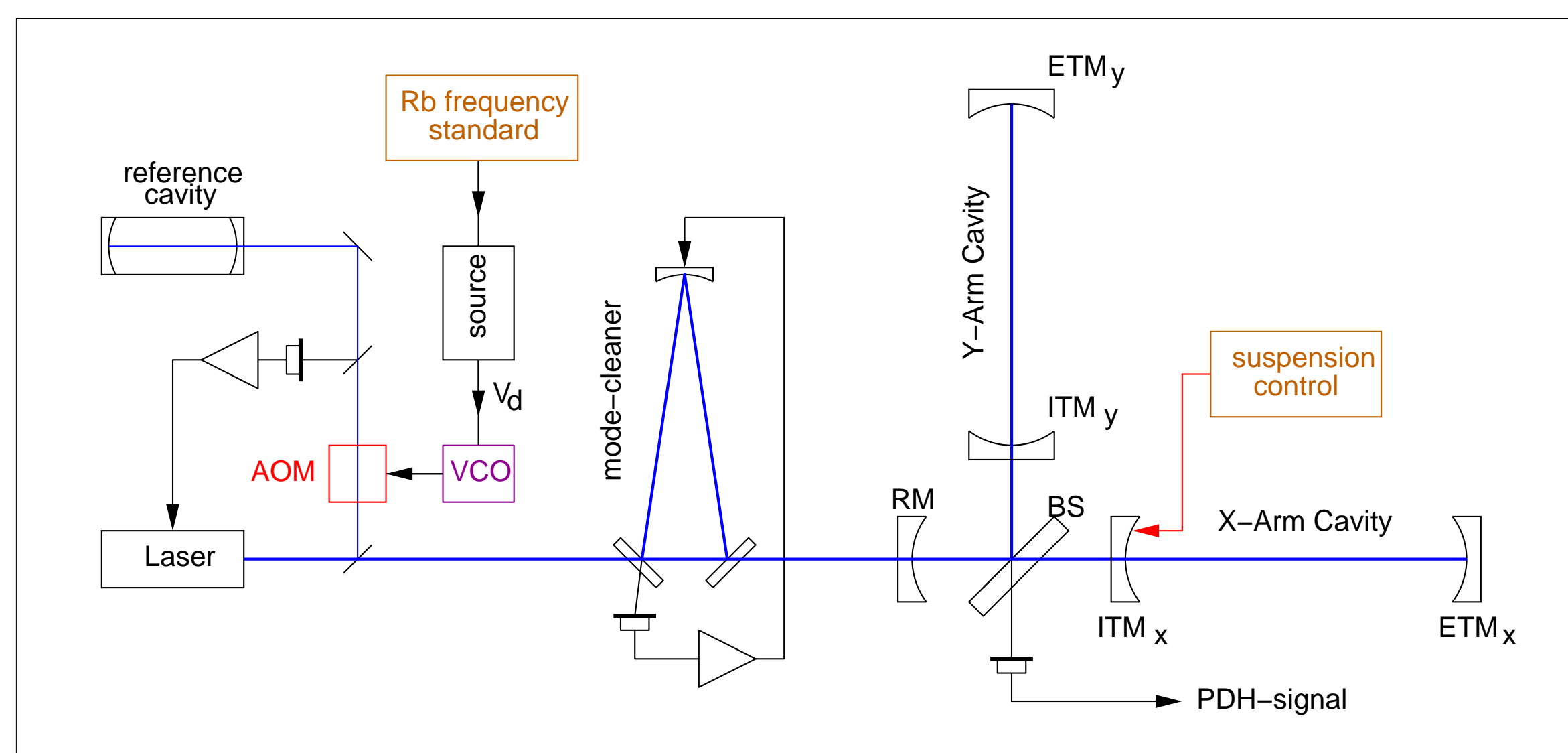
The Pound-Drever-Hall (PDH) locking signal, $V(t) = -\text{Im} \{ e^{i\gamma} (E_0 E_{-1}^* + E_1 E_0^*) \}$, is sensitive to deviations from this state of *dynamic resonance*. For small deviations from resonance, the PDH signal varies only slightly near its average value: $V(t) = \bar{V} + \delta V(t)$. The nominal operating point for the LIGO arm cavities is fringe center where $\bar{V} = 0$. Thus, the dynamic PDH signal, which has two components, can be written as $\delta V(t) = \delta V_0(t) + \delta V_1(t)$. The first term results from carrier field perturbations inside the cavity and the second term from sideband field perturbations inside the cavity:

$$\delta V_0(t) = -\text{Im} \left\{ e^{i\gamma} (\delta E_0 E_{-1}^* + E_1 \delta E_0^*) \right\}, \quad \delta V_1(t) = -\text{Im} \left\{ e^{i\gamma} (E_0 \delta E_{-1}^* + \delta E_1 E_0^*) \right\}.$$

We utilize the transfer functions between length or laser frequency variations and the dynamic PDH signal to investigate the properties of the LIGO 4-km-long Fabry-Perot cavities.

Experimental setup

To measure the laser frequency to PDH signal transfer functions, $H_\omega(s)$, we drive the VCO which controls the AOM that shifts the frequency of the laser light directed to the mode-cleaner as shown below. To measure the length to PDH signal transfer functions, $H_L(s)$, we drive the position of an input mirror via its suspension controller module. The PDH signals are measured at the anti-symmetric (AS) port of the interferometer. Precise frequency calibration is achieved via a benchtop Rubidium frequency standard (SRS model FS725).

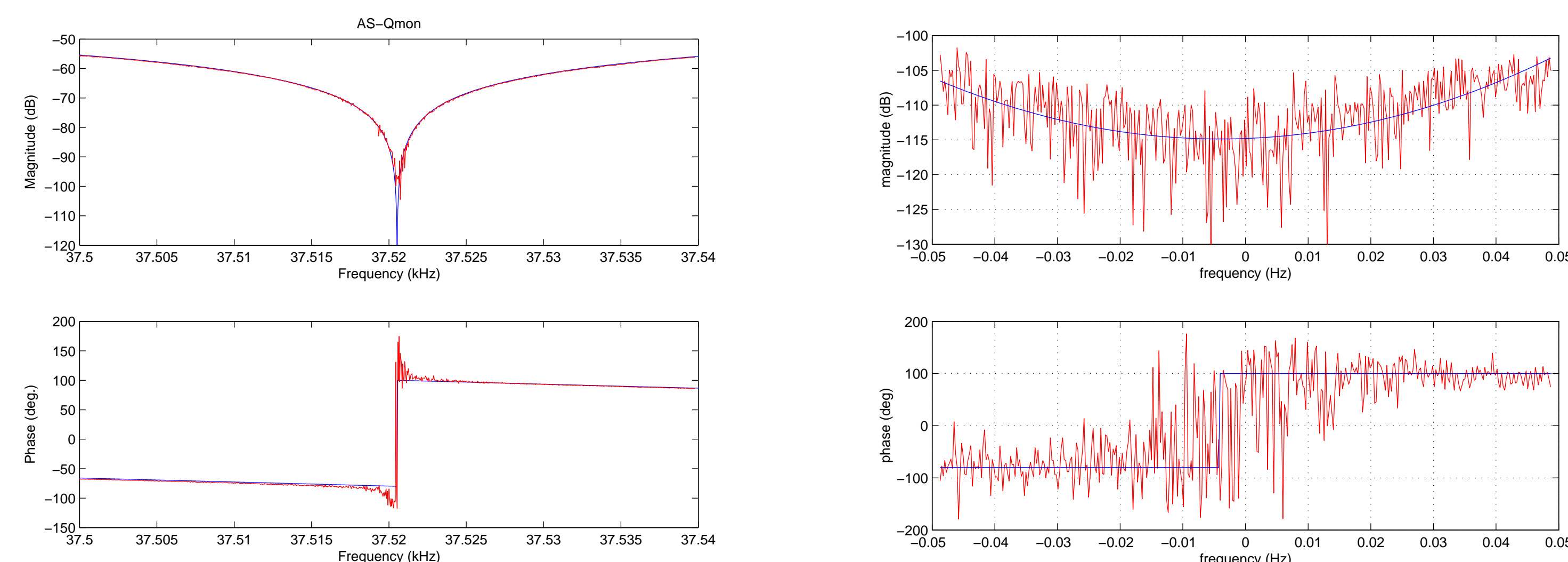


Response to laser frequency variations near the FSR

Near multiples of the cavity free spectral range (FSR), \tilde{V}_0 dominates and $H_\omega(s)$ is given explicitly by

$$\frac{\delta\tilde{V}_0(s)}{\delta\tilde{\omega}(s)} \equiv H_\omega(s) = C(s) H_L(s), \quad \text{where} \quad H_L(s) = \frac{1 - r_a r_b}{1 - r_a r_b e^{-2sT}}.$$

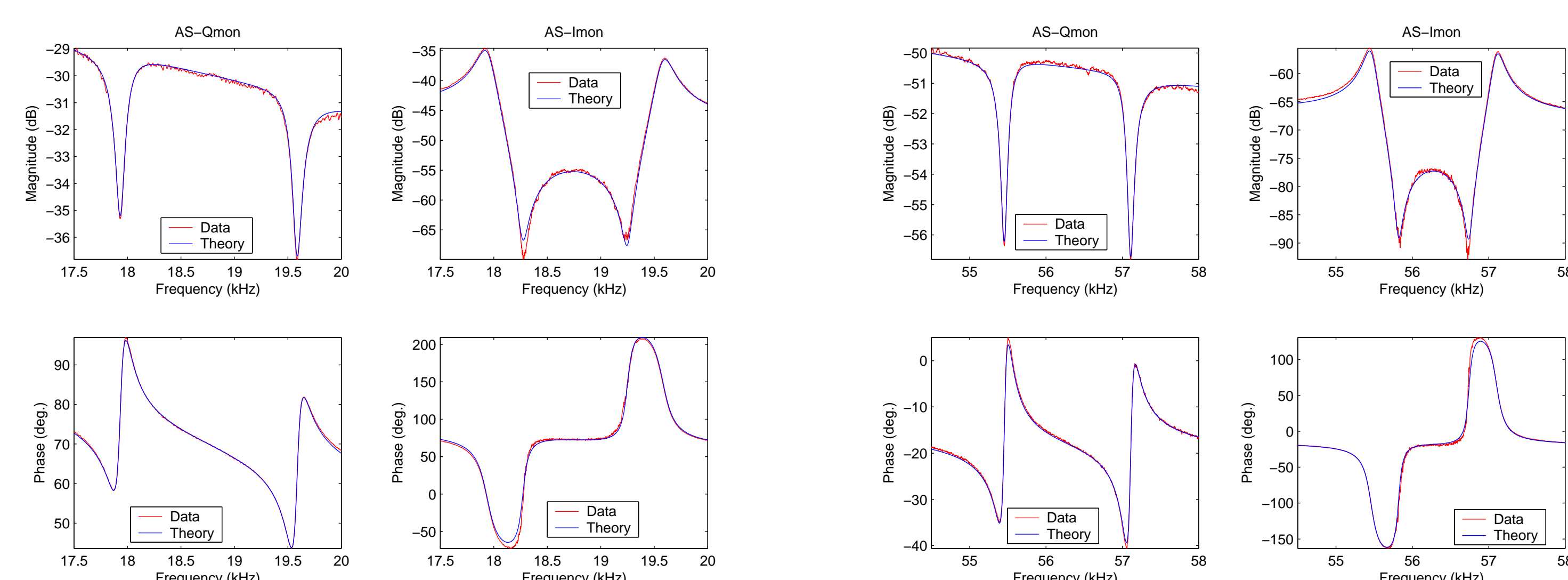
The measured transfer function, shown in both a wide frequency span (left) and a 0.1 Hz span (right) is in good agreement with the theoretical predictions.



Response to laser frequency variations near SB-related frequencies

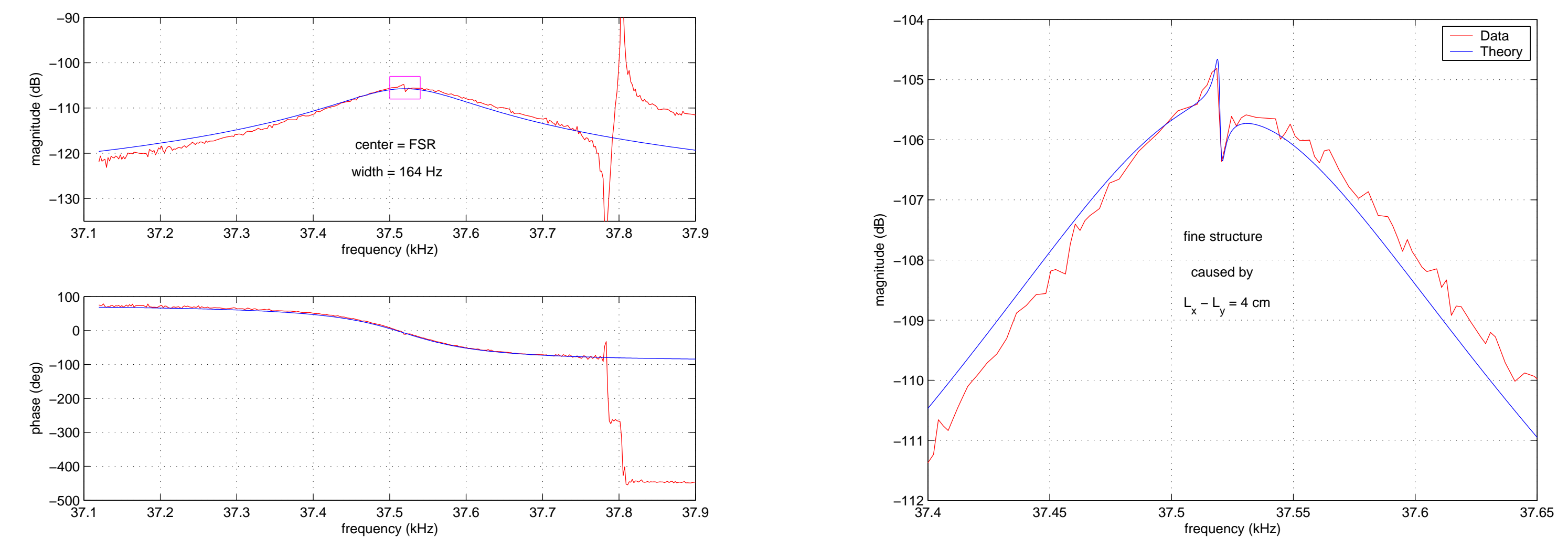
Near frequencies associated with the PDH phase modulation sidebands ($f_{\text{mod}} = 24,481,326$ Hz), the \tilde{V}_1 term generates features in the $H_\omega(s)$ transfer functions. The components of these double features appear symmetrically displaced from frequencies midway between multiples of the FSR.

The first plot group below shows features near 18.5 kHz and the second group shows features near 55.5 kHz, one FSR higher. Signals from both quadrature AS photodetector outputs, AS-Imon and AS-Qmon, are shown. By fitting the expression for $H_\omega(s)$ with the data, we estimate the Y-arm cavity length to be $L_Y = 3995.045 \pm 0.002$ m.



Response to cavity length variations near the FSR

The measured and predicted $H_L(s)$ transfer functions near the FSR are shown below. The response peaks as expected with a FWHM of about twice the cavity pole frequency. This transfer function, measured with the full interferometer locked while driving ITM_X exhibits a small wiggle near the peak. This feature is reproduced by both the *Finesse* and *e2e* models by introducing a 4 cm difference in the arm lengths (Y arm shorter).

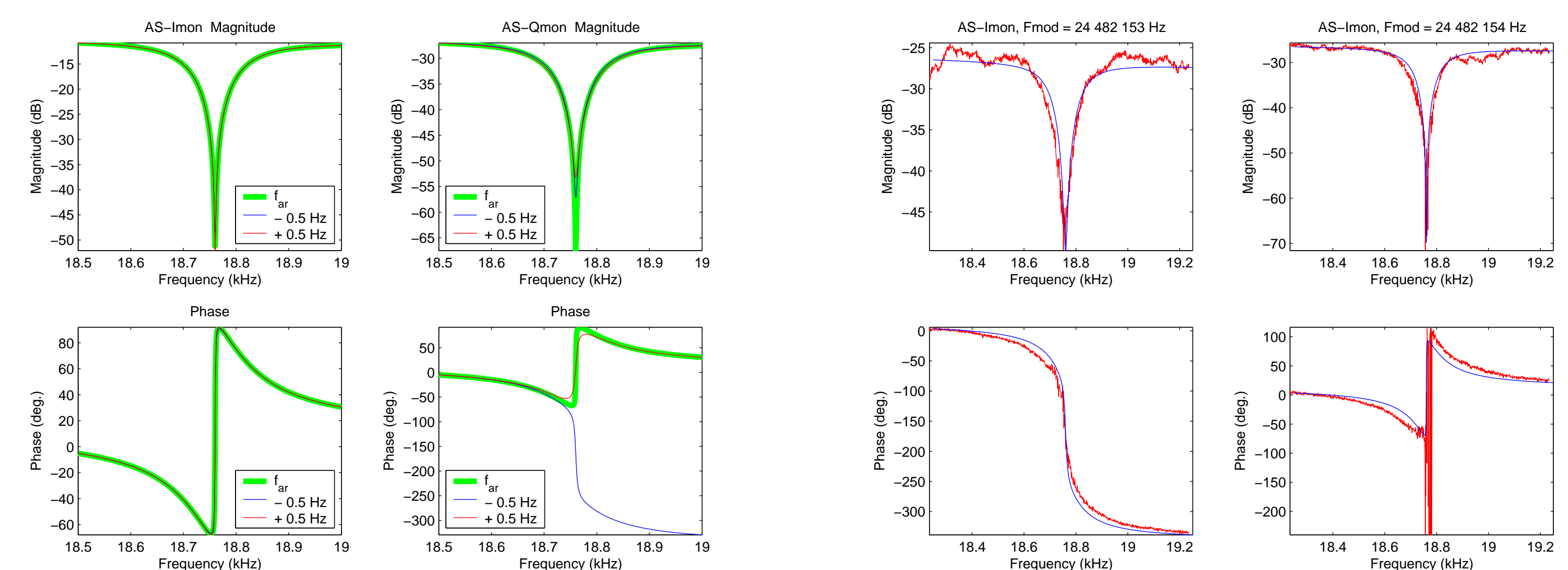


Precision measurement of the LIGO arm cavity lengths

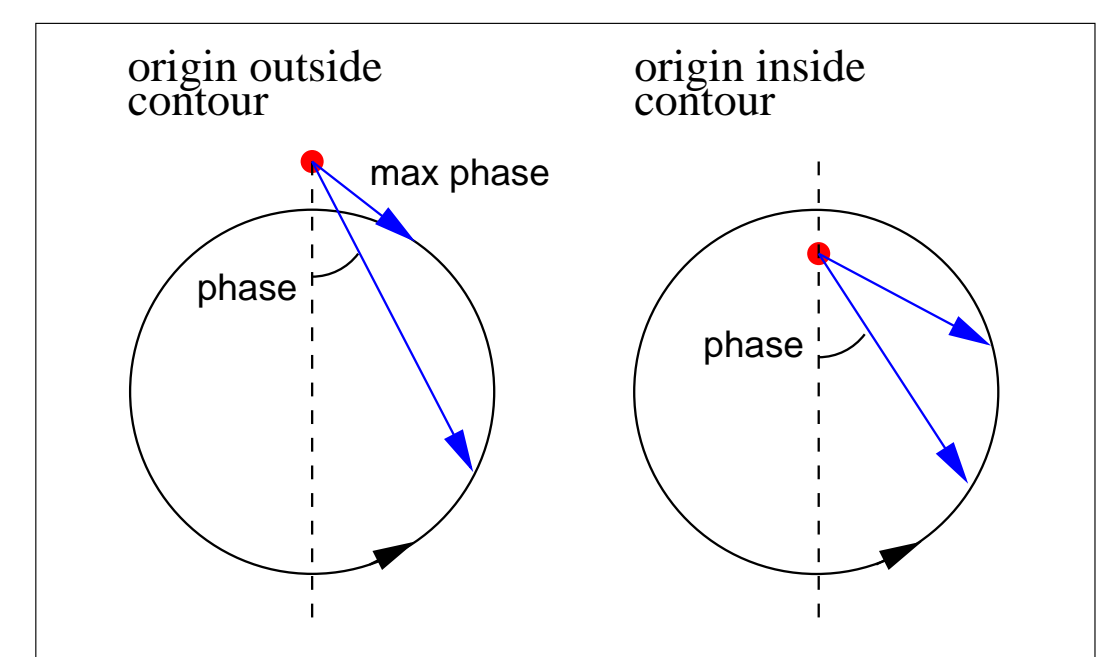
By tuning the PDH modulation frequency across the anti-resonance point (halfway between FSR peaks) we exploit an abrupt phase change in the $H_\omega(s)$ transfer function (bottom, right plot in the left figure group below) to precisely determine the arm lengths. Our precision is limited by the 1 Hz minimum step size of our f_{mod} frequency synthesizer. The bottom right plot group below shows the data for the Yarm transfer functions for a 1 Hz change in f_{mod} between the left and right columns. The cavity lengths thus measured are

$$L_X = 3995.08418 \text{ m} \pm 0.08 \text{ mm} \quad \text{and} \quad L_Y = 3995.04437 \text{ m} \pm 0.08 \text{ mm}.$$

The 39.81 mm arm length difference (Y arm shorter) is consistent with the $H_L(s)$ data above.

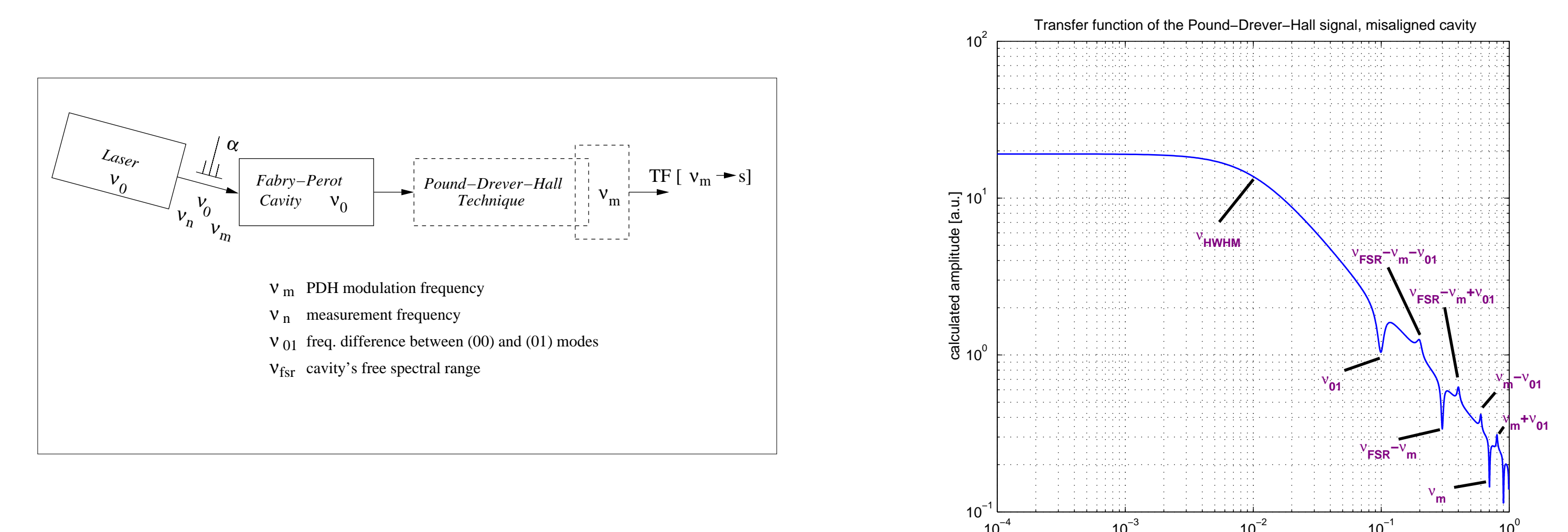


The abrupt change in the phase of the transfer function can be understood with the help of Nyquist diagrams, shown on the right. As the frequency changes, the tip of the phasor travels along a circular contour. If the origin is outside the contour the phase changes from 0 to some maximum value and back to 0. If the origin is inside the contour, the phase monotonically changes from 0 to 360° .



Measurement of mirror radius of curvature

When the laser beam entering the cavity is misaligned, features related to higher-order transverse modes appear in the $H_\omega(s)$ transfer function. These features are very similar to those produced by a cavity mode mismatch (except that the frequencies double). The size of the dips is proportional to the square of the misalignment.



An error signal, $\alpha = \left| \frac{\theta}{\theta_{\text{div}}} + i \frac{x}{w_0} \right|$, can be generated by demodulating at ν_{01} . If a monolithic photodiode is used, the magnitude of the signal is proportional to α^2 . With a split photodiode it can be proportional to α . These methods should be useful for monitoring changes in mirror radius of curvature (and g -factors) under high thermal loads. They may be used to predict servo instabilities which can occur for large misalignments or mode mismatches.

